Translational Cancer Mechanisms and Therapy

Clinical Cancer Research

Identification of Recurrent Activating *HER2* Mutations in Primary Canine Pulmonary Adenocarcinoma

Gwendolen Lorch[1], Karthigayini Sivaprakasam[2], Victoria Zismann[2], Nieves Perdigones[2], Tania Contente-Cuomo[2], Alexandra Nazareno[2], Salvatore Facista[2], Shukmei Wong[2], Kevin Drenner[2], Winnie S. Liang[2], Joseph M. Amann[3], Sara L. Sinicropi-Yao[3], Michael J. Koenig[3], Krista La Perle[4], Timothy G. Whitsett[2], Muhammed Murtaza[2], Jeffrey M. Trent[2], David P. Carbone[3], and William P.D. Hendricks[2]

Abstract

Purpose: Naturally occurring primary canine lung cancers share clinicopathologic features with human lung cancers in never-smokers, but the genetic underpinnings of canine lung cancer are unknown. We have charted the genomic landscape of canine lung cancer and performed functional characterization of novel, recurrent *HER2 (ERBB2)* mutations occurring in canine pulmonary adenocarcinoma (cPAC).

Experimental Design: We performed multiplatform genomic sequencing of 88 primary canine lung tumors or cell lines. Additionally, in cPAC cell lines, we performed functional characterization of HER2 signaling and evaluated mutation-dependent HER2 inhibitor drug dose-response.

Results: We discovered somatic, coding *HER2* point mutations in 38% of cPACs (28/74), but none in adenosquamous (cPASC, 0/11) or squamous cell (cPSCC, 0/3) carcinomas. The majority (93%) of *HER2* mutations were hotspot V659E transmembrane domain (TMD) mutations comparable to activating mutations at this same site in human cancer. Other *HER2* mutations were located in the extracellular domain and TMD. $HER2^{V659E}$ was detected in the plasma of 33% (2/6) of dogs with localized $HER2^{V659E}$ tumors. $HER2^{V659E}$ cPAC cell lines displayed constitutive phosphorylation of AKT and significantly higher sensitivity to the HER2 inhibitors lapatinib and neratinib relative to *HER2*-wild-type cell lines ($IC_{50} < 200$ nmol/L in $HER2^{V659E}$ vs. $IC_{50} > 2{,}500$ nmol/L in $HER2^{WT}$).

Conclusions: This study creates a foundation for molecular understanding of and drug development for canine lung cancer. These data also establish molecular contexts for comparative studies in dogs and humans of low mutation burden, never-smoker lung cancer, and mutant HER2 function and inhibition.

Introduction

Naturally occurring primary canine lung cancer is clinically challenging (1), with a disease course and underlying biology that resemble human lung cancer in never-smokers. Human never-smoker lung cancer accounts for 10% to 25% of lung cancers, causes approximately 26,000 deaths annually, and has a high incidence of erb-B family gene mutations such as those affecting *EGFR*. Although the incidence of smoking-related lung cancer is decreasing, lung cancer incidence in never-smokers is increasing (2). Never-smoker lung cancer is primarily non–small cell lung cancer (NSCLC), arising from lung tissue, as opposed to small cell lung cancer arising in bronchi of smokers. NSCLC histologies include adenocarcinoma (AC) and squamous cell carcinoma (SCC). The etiology of never-smoker lung cancer is also distinct from that of smokers. It is associated with factors including environmental exposures (secondhand smoke, radon, asbestos, arsenic, silica, and pollution) as well as age, sex, family history, and genetic loci (3). Unique genomic characteristics of human never-smoker lung cancer include low somatic mutation burden, enrichment for C:G>T:A transitions, and somatic activating point mutations or fusions affecting *EGFR* (45%), *ALK* (5%–11%), *ROS* (1.5%–6%), *HER2* (3%–5%), and *RET* (2%; ref. 4). The five-year overall survival is estimated at 23%, but outcomes are dependent on molecular subtype and treatment regimen. For example, EGFR inhibitors can improve outcomes in *EGFR*-mutant lung cancers; however, 85% of never-smoker lung AC and SCC cases are *EGFR* wild-type (WT) in the United States. Clinical trials of immune-checkpoint inhibitors have recently shown improved outcomes for human lung cancers, but analysis of large phase II immunotherapy trials suggests that benefits are limited in low-mutation-burden ($\leq$10 mutations/Mb) cases such

[1]Department of Veterinary Clinical Sciences, College of Veterinary Medicine, The Ohio State University, Columbus, Ohio. [2]Translational Genomics Research Institute, Phoenix, Arizona. [3]Department of Internal Medicine, James Thoracic Center, The Ohio State University, Columbus, Ohio. [4]Department of Veterinary Biosciences, Comparative Pathology and Mouse Phenotyping Shared Resource, College of Veterinary Medicine, The Ohio State University, Columbus, Ohio.

Note: Supplementary data for this article are available at Clinical Cancer Research Online (http://clincancerres.aacrjournals.org/).

Corresponding Author: William P.D. Hendricks, Translational Genomics Research Institute, 445 N 5th Street, Phoenix, AZ 85004. Phone: 602-343-8684; E-mail: WHendricks@tgen.org

Clin Cancer Res 2019;25:5866–77

doi: 10.1158/1078-0432.CCR-19-1145

Translational Relevance

We have discovered recurrent somatic *HER2 (ERBB2)* point mutations in 38% of cPACs that confer both constitutive activation of proliferative signaling and sensitivity to the HER2 inhibitors lapatinib and neratinib. These findings have relevance for veterinary oncology, comparative oncology, and the study of mutant HER2 inhibition.

as those found in never-smokers (5). A need exists for improved biological understanding and development of new models to fuel translational research in never-smoker lung cancer.

Lung cancer in pet dogs has limited standard of care beyond surgery, and little is known of its molecular underpinnings (1). Primary lung tumors typically arise in older dogs (11 years) and resemble human NSCLC histotypes including canine pulmonary adenocarcinoma (cPAC), adenosquamous carcinoma (cPASC), and SCC (cPSCC). These subtypes collectively represent 13% to 15% of primary lung tumors (6, 7). Patients are often diagnosed late with lesions incidentally discovered during routine geriatric evaluation or due to nonspecific symptoms including dyspnea (6%–24%) and cough (52%–93%) that do not manifest until the tumor is more than 3 cm. The detection of canine lung cancers has significantly increased over the past 20 years not only because of improved animal healthcare and diagnostics, but also possibly due to increased companion animal exposures to pollutants. These tumors can be diagnostically challenging. Rates at which ultrasound or CT-guided fine-needle aspirates of the pulmonary mass provide cytologic diagnosis range from 38% to 90% of cases, varying broadly based on tumor accessibility and aspirate quality. At diagnosis, 71% of malignant canine lung tumors show signs of invasion and 23% show distant metastasis. Partial or complete lung lobectomy is standard of care, dependent on the extent of disease spread. Median survival is 345 days for localized disease without nodal involvement where surgical remission can be achieved, but only 60 days when nodes are involved. Responses to cytotoxic chemotherapy (cisplatin, vindesine, doxorubicin, and mitoxantrone) in the setting of disseminated disease are limited. Targeted small molecules and immune-checkpoint inhibitors have not been extensively studied in part because the molecular underpinnings of canine lung cancer remain largely unknown. In naturally occurring canine NSCLC, although comprehensive genomic profiling has been limited, *KRAS* hotspot mutation prevalence estimates from targeted studies have varied from 0% to 25% (7–9). We have previously shown that EGFR mutation, overexpression, or phosphorylation is rare in cPAC compared with matched nonaffected chemotherapy-naïve lung tissue whereas significant overexpression and/or phosphorylation of PDGFRα, ALK, and HER2 are present (10). We now describe for the first time the detailed genetic underpinnings of primary canine lung cancers through multiplatform next-generation sequencing of 88 cases.

Materials and Methods

Sample collection

Tumors and cell lines from 89 dogs from the Canine Comparative Oncology and Genomics Consortium (CCOGC; ref. 11) and The Ohio State University (OSU) College of Veterinary Medicine Biospecimen Repository were included. Veterinary pathologists board certified by the American College of Veterinary Pathologists (ACVP) confirmed tumor diagnosis based on histopathology. This study was approved by The OSU Institutional Animal Care Use Committee (2010A0015-R2). Tumor and normal tissue samples were flash frozen in liquid nitrogen or formalin-fixed and paraffin-embedded (FFPE). Cell lines were received between May 29, 2017 (all sequenced lines), and May 18, 2018 (OSUK9-PAPADRiley), maintained in RPMI-1640 with GlutaMAX (Gibco, Thermo Fisher Scientific, #61870036) supplemented with 10% heat-inactivated fetal bovine serum at 37°C and 5% CO_2 and passaged at 90% confluence. Cell lines with known passage data (except BACA) were sequenced within the first eight passages of derivation, subsequently expanded for phenotypic studies, and authenticated by IDEXX BioResearch using the Cell Check Canine STR Profile and Interspecies Contamination Test on January 30, 2018, or by NkX2 (or *TTF-1*) RT-PCR. Mycoplasma testing was performed in all lines at time of arrival and every 3 months of continuous harvest by using the Mycoplasma Detection Kit (ATCC, #30-1012K). All samples tested negative at all times with final testing performed on June 21, 2019, for Riley and June 15, 2017, for all other lines). Human cell lines included BT474 (ATCC, #HTB20, *HER2* focal amplification) and H1781 (ATCC #CRL-5894, $HER2^{G776insV\_G/C}$). Blood for cell-free DNA and germline DNA extraction was collected in 10 mL K_2 EDTA Blood tubes (Thermo Fisher Scientific, #22-253-145). Plasma separation was performed at room temperature within 1 hour (2× serial centrifugation at 2000 rpm × 15 minutes). Plasma aliquots were stored frozen at −80°C. DNA extraction from plasma, white blood cells, and tissue was performed with MagMAX Cell-Free DNA Isolation Kit (Thermo Fisher Scientific, #A29319), DNeasy Blood and Tissue Kit (QIAGEN, #69504), and Qiagen AllPrep DNA/RNA Mini Kit (QIAGEN, #80204), respectively.

Exome sequencing and analysis

Informatic tools, versions, and flags are shown in Supplementary Table S1. We utilized a custom Agilent SureSelect canine exome capture kit with 982,789 probes covering 19,459 genes. Exome libraries were sequenced on the Illumina HiSeq2000 producing paired-end reads of 85 bp. FASTQ files were aligned to the canine genome (CanFam3.1) using BWA v0.7.8. Aligned BAM files were realigned and recalibrated using GATK v3.3.0, and duplicate pairs were marked with Picard v1.128 (http://broadinstitute.github.io/picard). Somatic copy-number variants (CNV) and structural variants (SV) were called with tCoNutT (https://github.com/tgen/tCoNuT) and DELLY v0.76, respectively. Somatic single-nucleotide variants (SNV) were identified from two or more of the following callers: Seurat v2.6, Strelka v1.0.13 and MuTect v1.1.4. Germline SNVs were called using Haplotype Caller (GATK v3.3.0), Freebayes, and samtools-Mpileup. Variant annotation was performed with SnpEff v3.5. The SomaticSignatures R package was used to identify mutation signatures.

Targeted amplicon sequencing and analysis

We developed a custom canine cancer amplicon sequencing panel consisting of 281 amplicons targeting exons and hotspot regions in 57 genes, with amplicon sizes ranging from 91 to 271 bp (Supplementary Table S7). We pooled primers in two multiplexed pools to separate adjacent amplicons and any amplicons that showed cross-amplification using *in silico* PCR. We prepared sequencing libraries using digital PCR amplification

following the manufacturer's protocols for the ThunderBolts Cancer Panel (RainDance Technologies) with modifications as previously described (12). Sequencing was performed on the Illumina MiSeq generating paired-end 275 bp reads. Sequencing reads were demultiplexed and extracted using Picardtools. Sequencing adapters were trimmed using ea-utils, and fastq files were assessed for quality using FASTQC. Sequencing reads were aligned to CanFam3.1 using bwamem-MEM (13). Custom in-house scripts based on samtools were used to create pileups for every sample. Pileups were analyzed in R to call SNVs and indels. For each potential nonreference allele at each targeted locus in a sample, we evaluated the distribution of background noise across all other sequenced samples. To call a variant, we required the observed nonreference allele to be an outlier within the background distribution with a *Z*-score > 5. In addition, we required tumor depth $\geq$100×, allele frequency $\geq$10%, number of reads supporting the variation $\geq$10, and allele fraction in the germline sample <1%. Finally, variant calls were manually curated by visualization in IGV v2.3.71. All next-generation sequencing data (exome and amplicon) have been deposited in the NCBI Sequence Read Archive repository under accession number PRJNA523624.

Sanger sequencing

Twenty-three primer pairs covering all exons of *HER2* were designed using Primer 3 (http://bioinfo.ut.ee/primer3-0.4.0/) including a universal M13 tag. Amplicons were Sanger sequenced at the DNASU sequencing facility at Arizona State University on an ABI 3730XL (Applied Biosystems) and analyzed with Mutation Surveyor DNA Variant Analysis Software (SoftGenetics).

HER2 inhibitor drug dose–response studies

The HER2 inhibitors lapatinib (Selleckchem, #S2111), neratinib (Puma Biotechnology, Los Angeles, CA), and trastuzumab (Selleckchem, #A2007), as well as the EGFR inhibitor erlotinib (Selleckchem, #S1023), were assessed in 10–16-point 72 hours drug-dose response screens (from 2×10^{-7} nmol/L to 100 μmol/L for small molecules and from 1×10^{-6} μg/mL to 1,000 μg/mL for trastuzumab) with CellTiter-Glo luminescent cell viability assay (Promega, #G7570) endpoints. Luminescence was read using a Synergy Mx (Biotek) plate reader. Six replicates were performed for each dose. Curve-fitting and IC_{50} calculations were performed using GraphPad Prism v7.00 (GraphPad Software).

Droplet digital PCR for cell-free DNA analysis

HER2^{V659E} genotyping was performed on tumor samples and plasma cell-free DNA with droplet digital PCR (ddPCR). PCR amplification was performed as follows: 1 cycle 3 minutes at 95°C, 50 cycles 15 seconds at 95°C and 1 minute at 60°C with a 0.5°C/second ramping from 95°C to 60°C, 1 cycle 98°C for 10 minutes and hold at 4°C. Droplet fluorescence was measured using RainDrop Digital PCR Sense instrument and analyzed using accompanying RainDrop Analyst II Software v.1.0 (RainDance). Primer and probe sequences used for *HER2*^{V659E} detection in ctDNA were forward: 5′-CCCACGACCACAGCCA-3′, reverse: 5′-CCCTGTGACATCCATCATTGC-3′, and probe: 5′-CAGAATGCCC (T/A)CCACAGC-3′.

qRT-PCR

cDNA was obtained by reverse transcription with iScript (Bio-Rad, #1708891) and samples were subjected to *HER2* (target) and *HPRT1* (reference) amplification in a QuantStudio 6 Flex Real-Time PCR System under standard conditions with Syber Green technology (KapaBiosystems, #KK4602). Primer sequences were: *HER2*-forward: 5′-CATCTGCACCATTGATG-TCTA-3′, *HER2*-reverse: 5′-GGCCCAAGTCTTCATTCTGA-3′, *HPRT1*-forward: 5′GCAGCCCCAGCGTCGTGATT-3′, *HPRT1*-reverse: 5′CATCTCGAGCAAGCCGCTCAGT-3′. Data were analyzed with Quantstudio Real-Time PCR software v1.1. Values for ΔCt, ΔΔCt, and fold changes were calculated as follows: ΔCt = Ct HER2 − Ct HPRT1; ΔΔCt = ΔCt tumor sample – ΔCt average of normal samples; and fold change = $2^{(-\Delta\Delta Ct)}$.

Immunohistochemistry

HER2 protein expression was evaluated on FFPE sections (4 μm) of normal lung and tumor mounted on SuperFrost Plus glass slides (Fisher Scientific, #12-550-15). Slides were deparaffinized in xylene and rehydrated in an ethanol gradient. Antigen retrieval was performed with 1 mmol/L EDTA adjusted to pH 9.0. An autostainer (Dako, model S3400) was used to carry out immunostaining. A HER2 rabbit monoclonal antibody (Cell Signaling Technology, #4290) was used at 1:400 dilution followed by secondary biotinylated rabbit anti-goat IgG (Vector Laboratories, BA-1000) diluted 1:200. Detection was performed with VECTASTAIN Elite ABC System (#PK-6100). IHC-positive controls for HER2 tyrosine kinase receptor expression were single tissue samples of two canine complex mammary carcinomas (14). Negative controls were performed on all tissues using a universal rabbit negative isotype control not directed against any known antigen (Dako, #IR600).

Quantitative image analysis

Immunostained and control 1 × 3-inch microscope slides were scanned at 40× on a high-resolution Scanscope XT (Leica Biosystems) at The OSU Comparative Pathology and Mouse Phenotyping Shared Resource. For the quantification of immunoreactivity, images were imported into Visiopharm Image Analysis software (Visiopharm, Hørsholm, Denmark version 2017.27.0.3313), segmented into areas of tumor, necrosis, and normal lung tissue using color labels for each tissue type. HER2 connectivity was scored using the modified 10007-HER2, Breast Cancer APP (Visiopharm). Thresholds were adjusted to match specimen HER2 stain intensities for accurate scoring. Area (μm^2) was quantified for each tissue type, and percentages were derived from specimen total tissue area. Tumor areas were further segmented into staining and non-staining categories, and their percentages were calculated based on the total tumor area in μm^2. Maximum, mean, and minimum intensities were also quantified using a built-in software calculation. Staining is expressed as a percentage of stain present with 100% equal to black (maximum dark brown) and 0% equal to white (no stain present). Initial thresholds and tissue types were established, and mark-ups were reviewed in consultation with a pathologist board-certified by the ACVP to ensure accurate measurements and to differentiate between tissue types.

Immunoblot analyses

Subconfluent cells were serum starved overnight, and then treated with 20 nmol/L neuregulin for 15 minutes prior to harvest. Cells were lysed in RIPA buffer with cOmplete Mini Protease Inhibitor (Roche, #11836153001) and PhosSTOP (Roche, #4906845001) and loaded in Laemmli buffer at

1 μg/μL. Samples were separated on 4% to 15% SDS-PAGE Criterion Gels (Bio-Rad, #5671085) and transferred to Immobilon-FL PVDF membrane (MilliporeSigma, #IEVH7850). Membranes were blocked for 1 hour in LI-COR blocking buffer and incubated with primary antibody at 4°C overnight, followed by fluorescence-conjugated secondary antibodies. Membranes were scanned using the LI-COR Odyssey CLx instrument. Primary antibodies were AKT (CST #4691S, 1:1,000), phospho-AKT (CST #4060P, 1:1,000), and β-actin (CST #4970S, 1:1,000).

Results

The genomic landscape of naturally occurring primary canine lung cancer

In order to map the genomic landscape of primary canine lung cancer, we undertook multiplatform next-generation sequencing of 88 NSCLC cases, including 78 tumor/normal matched pairs and 10 cell lines (Table 1). The cohort included 74 cPAC, 11 cPASC, and 3 cPSCC. Labrador retrievers represented the most commonly affected pure breed dog (21%) with mixed breeds (25%) and multiple other single pure breeds. The predominant cPAC subtype was papillary adenocarcinoma (62%). The cohort was gender balanced (52% females) and primarily neutered/spayed (92%) with a median age at diagnosis of 11 years. Smoking status in the pet's household was not available. Extended clinical annotation is shown in Supplementary Table S2 and Supplementary Fig. S1.

To identify somatic point mutations, copy-number changes, and translocations, we first performed exome sequencing of five cPAC tumors and matching normal samples with a mean target coverage of 298× and 263×, respectively (99% of target bases covered ≥ 40×, Supplementary Table S3). A total of 648 high-confidence somatic SNVs (median 64; range, 37–406), 165 focal CNVs (median 19; range, 0–116), and 3 SVs (median 1; range, 0–1) were identified (Supplementary Tables S4–S6; Fig. 1A–C). The average tumor mutation burden (TMB) for somatic point mutations per haploid callable megabase (Mb) in these cases was 2.04 mutations/Mb (range, 0.58–6.38). Among these somatic variants, we identified mutations in genes whose human orthologs have been implicated in human cancer according to COSMIC (15) tiers 1 and 2, including somatic SNVs (Supplementary Table S4), focal CNVs (Fig. 1B; Supplementary Table S5), SVs, and numerical chromosomal changes (whole chromosome or arm-level gains/losses; Supplementary Fig. S2). The sole gene bearing recurrent nonsynonymous SNVs was *HER2* (80%), with the missense mutation V659E occurring in three cases and the missense mutation K676E in a fourth case (Fig. 1D). No *HER2* amplifications were detected in these five tumors. We also assessed somatic point mutation signatures according to their trinucleotide context (Supplementary Fig. S3; refs. 16, 17). The most common signature in these five cases was the age-associated COSMIC Signature 1A in four of five (80%) and COSMIC signature 2, associated with APOBEC cytidine deaminase activity, in two cases.

Table 1. Genomic analyses performed in primary canine lung cancer

Analysis platform	Sample analyzed[a]	Type of alteration detected
Exome	5 cPAC and matching normal	Germline and somatic SNVs, CNVs, and SVs in coding regions
Amplicon	61 cPAC and matching normal[b], 8 cell lines	Germline and somatic SNVs in 53 cancer genes
	10 cPASC and matching normal, 1 cell line	Germline and somatic SNVs in 53 cancer genes
	2 cPSCC and matching normal, 1 cell line	Germline and somatic SNVs in 53 cancer genes
Total	**78 tumor–normal pairs, 10 cell lines**	

Abbreviations: cPASC, canine pulmonary adenosquamous carcinoma; cPSCC, canine pulmonary squamous cell carcinoma.

[a]An additional cell line (OSUK9PADRiley) was analyzed by Sanger sequencing.
[b]All matching normal samples were available except one (CCB30381).

To identify somatic point mutations across a broader cohort of canine lung cancers, we used a custom canine cancer amplicon-based sequencing panel (Supplementary Table S7) in 73 additional lung tumors (61 cPAC, 10 cPASC, and 2 cPSCC), two previously exome-sequenced tumors with matched normal tissue, and 10 cell lines (8 cPAC, 1 cPASC, and 1 cPSCC). These cases were sequenced to an average depth of 3,383× (Supplementary Table S8). A median of 1 somatic coding point mutation (range, 0–3) within sequenced panel regions was identified across all cases. Likely pathogenic recurrent point mutations included *HER2* V659E (29.8%), *KRAS* G12D/V (3.4%), *SMAD4* D351Y/G (3.4%), and *TP53* R239Q/G (2.2%; Supplementary Table S9). Two additional somatic missense mutations in *HER2* were identified in single cases (Fig. 1D). Overall, recurrently mutated genes containing somatic potentially pathogenic SNVs included *TP53* (12.5%), *PTEN* (5.7%), *SMAD4* (4.5%), *KRAS* (4.5%), *VHL* (3.4%) and *HRAS* (2.3%). Finally, based on both exome and amplicon sequencing, we evaluated germline SNPs to identify putatively pathogenic rare variants (i.e., those not previously identified in dogs based on review of presence in dbSNP 151, ref. 18; and/or ≥10% frequency in DogSD, ref. 19) in 81 genes potentially associated with susceptibility to human lung cancer (20). We identified nine rare putatively pathogenic SNPs in five dogs in the genes *CHRNA3*, *CYP1B1*, *DNAH11*, and *HER2* (Supplementary Table S10). Of these SNPs, the only variant with an equivalent in its human orthologous gene was *DNAH11* R1460W corresponding to human *DNAH11* R1444W (rs1035326227, Minor Allele Frequency < 0.01%). The human SNP has not been associated with disease. *HER2* V1189I variants occurred in two cases without somatic *HER2* tumor mutations. The human orthologous position V1184 has not shown human variation. The canine variant has been identified in 4% of cases in DogSD and based on functional effect prediction (FATHMM), it is likely neutral. None of the genes bearing rare SNPs showed second hits in tumor tissue.

We additionally performed matched tumor/normal amplicon sequencing to evaluate the genomic landscapes of 11 cPASC and 3 cPSCCs, subtypes that are understudied entities in dogs and humans, especially in never-smokers (Fig. 1A; Supplementary Table S9). In contrast with cPAC, no *HER2* mutations were identified in these tumors. In cPASC, *HRAS* Q61L and *KRAS* Q61K each occurred in one case. Thus, 18% of cases bore *RAS* hotspot mutations. *PTEN* stop gains additionally occurred in two of 11 (18%) of cases at high tumor allele frequencies and were exclusive with *RAS* mutations. Additional likely pathogenic somatic mutations also occurred in a single cancer gene in a single tumor each including *EGFR* A726T, *MET* M1269V, *TP53* R147C, and *VHL* P97L. Finally, although no recurrent mutations were identified in the three cPSCCs, we identified one case with a somatic *BRAF* V588E and another bearing *PTPN11* G503V.

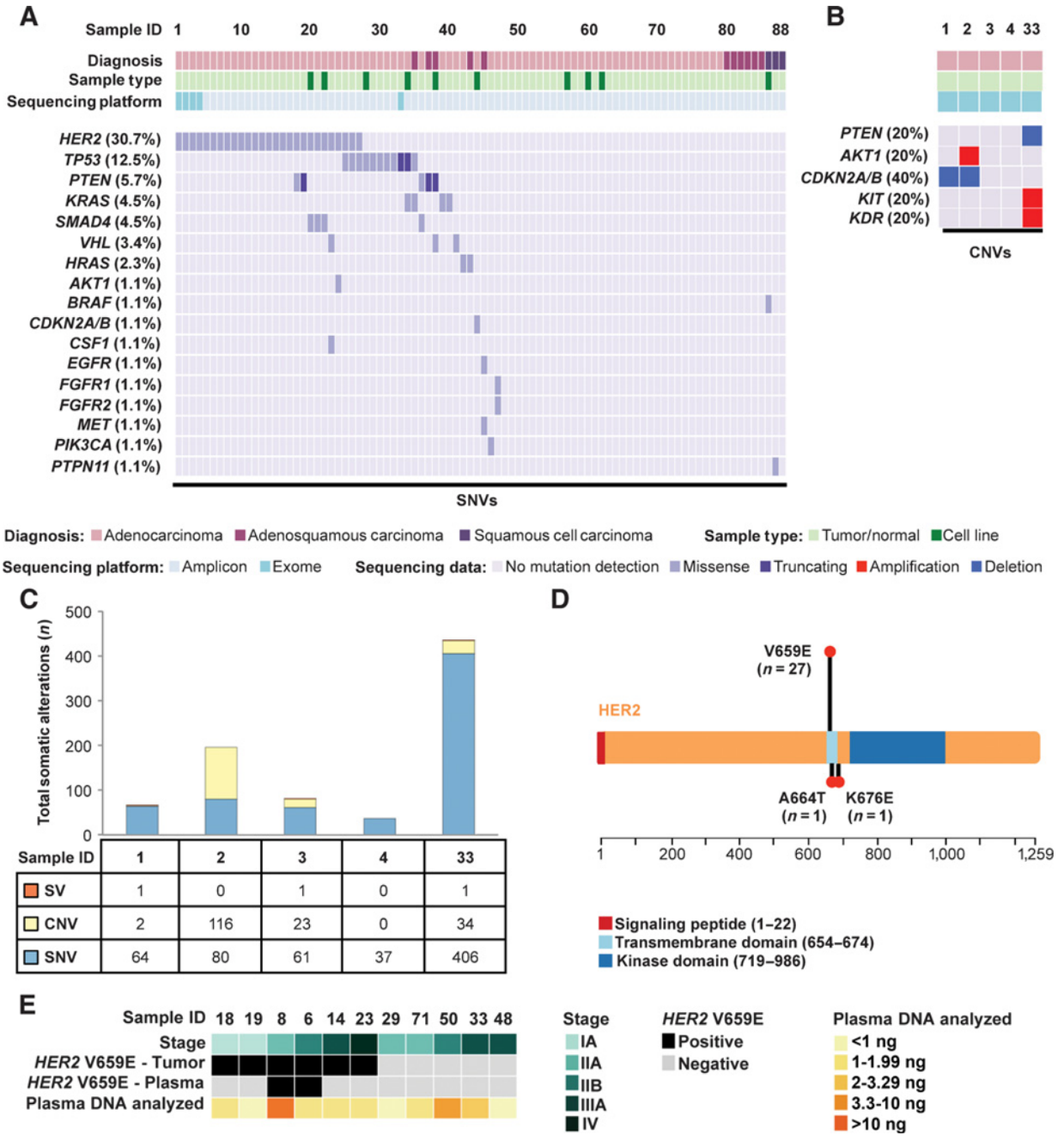

Figure 1.

The genomic landscape of primary canine lung cancers. **A,** Recurrent likely pathogenic somatic mutations in cancer genes identified in primary canine lung cancers through multiplatform sequencing. SNVs were determined from combined tumor/normal exome and/or amplicon sequencing across 88 total tumors and cell lines. **B,** CNVs were determined from tumor/normal exome data in five cPAC cases. **C,** Somatic mutation burden (SNVs, CNVs, and SVs) identified by exome sequencing of five tumor/normal cPAC cases. **D,** Distribution of somatic *HER2* mutations within the HER2 protein identified in primary canine lung cancers. The length of the lollipops is proportional to the number of mutations found. **E,** Detection of *HER2* hotspot mutations in plasma from 11 canine primary lung cancer cases.

Frequent *HER2* mutation in cPAC

HER2 was the most frequently mutated gene in our multiplatform next-generation sequencing cohort, with missense mutations occurring exclusively in cPACs (27/74, 36.5%, two mutations occurring in a single patient; Fig. 1A). No *HER2* insertions were identified. We additionally identified a *HER2* mutation in the cell line OSUK9PAPADRiley solely by Sanger sequencing of the codon 659 locus. We thus identified 29 total *HER2* mutations overall (Fig. 1D). In 24 cases, the *HER2* variants were evaluated on at least two platforms, including exome sequencing, amplicon

sequencing, Sanger sequencing, and/or ddPCR (Supplementary Table S11). The *HER2* variant tumor allele fraction (AF) median by amplicon sequencing was 21.3% (range, 8.4%–51.9%). All low AF (<20%) cases identified by amplicon sequencing were also validated by Sanger and/or ddPCR. Notably, one cell line, OSUK9PAPADOscar, contained a low AF *HER2* V659E variant (AFs of 15% by amplicon and 16% by ddPCR) during early short-term culture (passage 4) that was no longer detectable by Sanger sequencing or ddPCR in later passages (passage 15). Importantly, passage 15 was utilized for all functional studies described below, and it was thus considered $HER2^{WT}$ in this setting. Overall, V659E missense mutations located in the HER2 TMD occurred in 93.3% of *HER2*-mutant cases. Additional *HER2* mutations included A664T (OSU419040) and K676E (CCB050354), which have not been previously described in orthologous human *HER2* regions. In some cases, *HER2* mutations co-occurred with mutations in *TP53*, *SMAD4*, *PTEN*, *VHL*, *AKT1*, or *KDR*.

Detection of *HER2* mutations in canine plasma DNA

Cell-free tumor DNA (ctDNA) in plasma has been increasingly used for noninvasive genotyping in human cancer patients (21). To develop a canine blood test that could rapidly identify dogs with *HER2*-mutant lung cancer, we investigated whether cPAC *HER2* hotspot mutations are detectable in ctDNA. We evaluated plasma from 11 dogs—5 with $HER2^{WT}$ tumors and 6 with $HER2^{V659E}$ tumors—using ddPCR (Supplementary Table S12). In order to evaluate assay performance (specificity), we first analyzed WT tumor samples, plasma DNA from unrelated commercially available canine plasma samples, and template-free controls (BioreclamationIVT, #BGLPLEDTA-100-P-m). Using uniform gating for all experiments, we found one of seven template-free samples showed one WT droplet and no samples showed any evidence of mutant DNA amplification. In WT tumor and plasma DNA samples, two of eight samples showed one mutant droplet each. Based on these results, we required at least three mutant droplets to confidently detect $HER2^{V659E}$. To confirm mutation detection and quantitative performance, we analyzed and detected $HER2^{V659E}$ in six of six positive control tumor DNA samples where we had previously identified V659E mutations using amplicon sequencing. In these samples, we observed a high correlation between AFs measured using amplicon sequencing and ddPCR (Pearson r 0.976, $P = 0.0008$; Supplementary Fig. S4). In 11 plasma samples from dogs with cPAC tested using ddPCR, the median total cell-free DNA (cfDNA) concentration was 3.7 ng/mL plasma (range, 0.7–23.0; Supplementary Table S12). Requiring at least three mutant droplets to support mutation detection and testing cfDNA equivalent to 435 μL plasma, the median limit of detection for mutation allele fraction was calculated at 0.61% (range, 0.10%–3.11%). $HER2^{V659E}$ mutations were detected in two of six plasma samples from dogs with $HER2^{V659E}$-positive tumors at 1.9% and 2.3% allele fractions. $HER2^{V659E}$ was not detected in any plasma samples from dogs with $HER2^{WT}$ tumors, confirming assay specificity (Fig. 1E). Sensitivity for mutation detection in this cohort may be limited due to low total cfDNA concentration and amounts analyzed.

HER2 expression in primary canine lung cancer

In human cancers, *HER2* bears activating point mutations, copy-number gains/amplifications, and RNA and protein overexpression. Amplification and overexpression are typically mutually exclusive with point mutations. *HER2* copy number was first determined in the five exome-sequenced cases (Supplementary Fig. S2; Supplementary Table S5). No numerical CFA9 gains or focal *HER2* amplifications were detected. However, these cases predominantly bore somatic putatively activating point mutations and might not be expected to contain concomitant gains. Therefore, we evaluated HER2 RNA and protein expression by qRT-PCR and IHC. RNA samples from 49 lung tumors (nine *HER2* mutant) were evaluated alongside 14 normal lung tissue samples distal to tumor areas but from the same lung lobe. Median HER2 expression fold change relative to expression of the housekeeping gene *HPRT* in normal lung samples was 1.06 (range, 0.28–4.11) and in tumors was 0.85 (range, 0.07–4.50; Supplementary Fig. S5). No significant difference in relative HER2 expression was observed between tumor and normal or *HER2*-mutant and $HER2^{WT}$ groups.

Additionally, in order to quantify HER2 protein expression in cPAC, digital image analysis was performed on eight tumors from FFPE. Three of the samples bore the $HER2^{V659E}$ hotspot mutations, one bore $HER2^{A664T}$, and four were $HER2^{WT}$. All cases were positive for HER2 staining with homogeneous and diffuse staining of tumor cell cytoplasm and cell membrane, but no staining in adjacent stroma or vasculature (Supplementary Fig. S6). Positive staining was observed in bronchial epithelium of the adjacent nonaffected lung in all cases. Consistent with the absence of observed *HER2* amplifications, no significant differences (mean ± SEM) were detected in the tumor positivity percentage for HER2 (47 ± 5.4 and 35 ± 5.1) between the WT and *HER2*-mutant groups, respectively. No significant differences in HER2 staining were present for percent minimum (51 ± 2.9 WT vs. 55 ± 5.1, *HER2* mutations) or percent maximum (97 ± 0.31 WT vs. 96 ± 0.47 *HER2* mutations) stain intensity (Supplementary Table S13). Overall, most tumors showed moderate expression of HER2 based on qRT-PCR and IHC with some variability, but levels were typically consistent with those seen in normal tissue and did not vary based on *HER2* mutation status.

Constitutive HER2 activation in $HER2^{V659E}$ cPAC cell lines

HER2 is a transmembrane receptor tyrosine kinase typically activated by homodimerization or heterodimerization with other HER family receptors. HER2 mutations or overexpression drive constitutive downstream signaling. In human cancers, *HER2* V659E mutations stabilize dimers to increase HER2 autophosphorylation, EGFR phosphorylation, activation of phosphatidylinositol-3-kinase (PI3K), and activation of mitogen-activated-protein-kinase (MAPK) prosurvival signaling pathway members (e.g., AKT and ERK) relative to WT *HER2* (22, 23). To determine whether $HER2^{V659E}$ constitutively activates downstream signaling in cPAC, we first validated *HER2* genotype in seven canine lung cancer cell lines through amplicon sequencing, ddPCR, or Sanger sequencing of the V659 locus, Sanger sequencing of all HER2 coding regions, and/or aCGH to determine *HER2* copy-number status as previously published (Supplementary Table S11; ref. 24). One cell line, OSUK9PAPADOscar, bore a low allele frequency $HER2^{V659E}$ mutation when sequenced by an amplicon panel at low passage (passage 4) as a primary culture, but had lost this allele in later established passages (passage 15) characterized by Sanger sequencing and ddPCR. The latter passages were utilized for functional studies. We thus evaluated HER2 activation in one $HER2^{V659E}$ cPAC cell line, OSUK9PAPADRex, and three $HER2^{WT}$ cell lines (two cPAC: CLAC and OSUK9PAPAPADOscar; and one

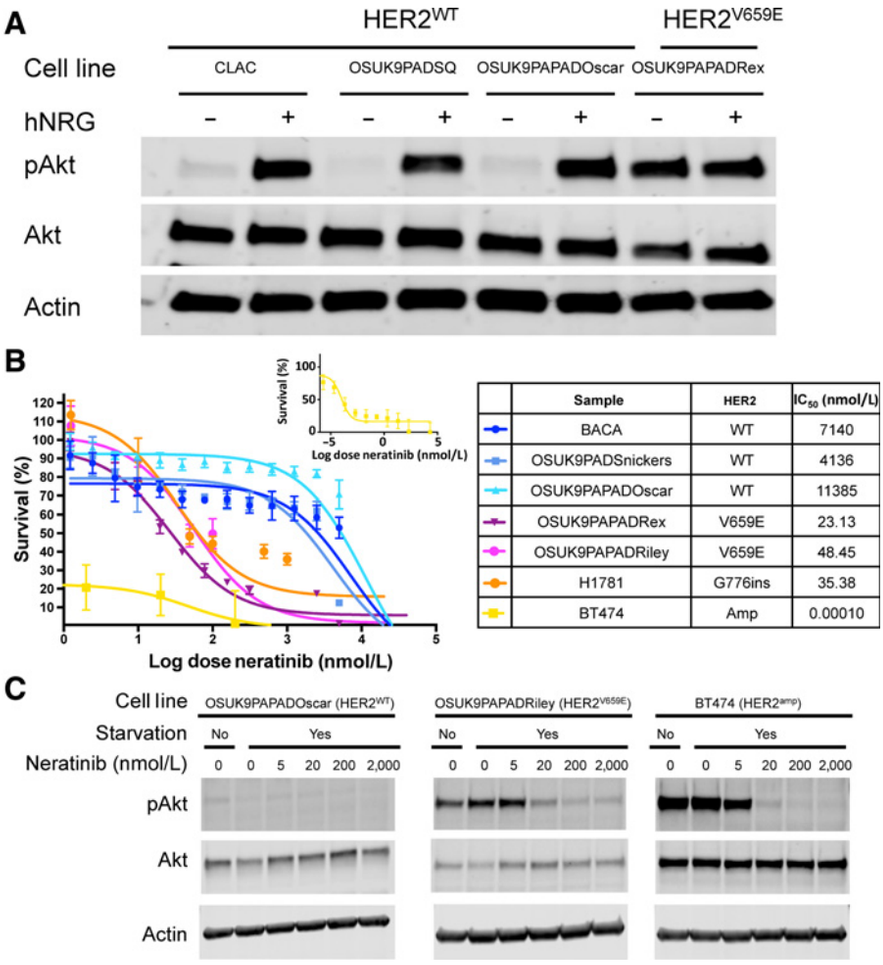

Figure 2.
HER2^{V659E} constitutively activates downstream HER2 signaling and is associated with response to HER2 inhibitors in primary cPAC cell lines. **A,** HER2 signaling activation in canine lung cancer cell lines. Phospho-AKT and AKT levels were assessed by Western blot under serum starvation in the presence and absence of EGFR activation by hNRG in *HER2*^{V659E} and *HER2*^{WT} cPAC cell lines. **B,** Neratinib drug dose–response studies in primary lung cancer cell lines. Five canine cell lines (three *HER2*^{WT} and two *HER2*^{V659E}) and two human lung cancer positive controls with known *HER2* activating mutations (BT474: *HER2*-amplified; H1781: *HER2*$^{G776insV\_G/C}$) and HER2 inhibitor responses were treated with 14 neratinib doses ranging from 100 μmol/L to 5.5×10^{-2} nmol/L for 72 hours with CellTiter-Glo viability endpoints. Survival is shown relative to DMSO vehicle control. **C,** Dose effect of the HER2 inhibitor neratinib on downstream AKT activation. Phospho-AKT and AKT levels were assessed in two canine lung cancer cell lines – OSUK9PAPADOscar (*HER2*^{WT}) and OSUK9PAPADRiley (*HER2*^{V659E}) – and compared to a well-characterized human lung cancer cell line (BT474, *HER2*-amplified) by Western blot under serum starvation in the presence of 5 doses (20–2000 nmol/L) of neratinib.

cPASC: OSUK9PADSQ) by Western blotting for total and phospho-AKT in the presence and absence of the ErbB ligand, neuregulin (hNRG) post-serum starvation. Only the *HER2*^{V659E} line OSUK9PAPADRex showed constitutively high AKT phosphorylation post-starvation even in the absence of hNRG stimulation (Fig. 2A).

Selective sensitivity of *HER2*^{V659E} cPAC cell lines to HER2 inhibitors

To determine the potential efficacy of anti-HER2 agents for treatment of *HER2*^{V659E} cPAC, we performed dose–response studies of selected tyrosine kinase inhibitors (TKI: neratinib, lapatinib, and erlotinib) and a humanized HER2 recombinant monoclonal antibody (mAb), trastuzumab, which binds the extracellular juxtamembrane domain IV of HER2. We first assessed the differential sensitivity of *HER2*^{V659E} and *HER2*^{WT} canine lung cancer cell lines to lapatinib (HER2 and EGFR inhibitor) and neratinib (HER2, HER4, and EGFR inhibitor). Five cPAC cell lines (two *HER2*^{V659E} and three *HER2*^{WT}) were treated with neratinib and four (one *HER2*^{V659E} and three *HER2*^{WT}) with lapatinib for 72 hours. Two *HER2*-mutant human cancer cell lines—BT474 (*HER2*^{AMP}) and H1781 (kinase domain *HER2*$^{G776insV\_G/C}$)—were treated as positive drug controls (refs. 22, 25; Fig. 2B; Supplementary Fig. S7). Significant differences in viability were observed between *HER2*^{V659E} and *HER2*^{WT} cPAC cell lines for both TKIs (IC_{50} < 200 nmol/L in *HER2*^{V659E} *vs.* IC_{50} > 2,500 nmol/L in *HER2*^{WT}). All *HER2*-mutant cell lines were sensitive to neratinib with IC_{50} < 50 nmol/L (Fig. 2B), significantly lower than those observed for *HER2*^{WT} cells (IC_{50} > 2.7 μmol/L, $P = 0.0079$). We additionally observed a neratinib dose-dependent decrease in p-AKT in the *HER2*-mutant cell lines OSUK9PAPADRiley (*HER2*^{V659E}) and BT474 (*HER2*^{amp}), whereas p-AKT levels in OSUK9PAPADOscar (*HER2*^{WT}) were low at all treatment levels (Fig. 2C). Given that HER2 receptors dimerize with EGFR, we then evaluated differential sensitivity of the five canine cell lines and the human BT474 control line to the EGFR inhibitor erlotinib. Not surprisingly, *HER2*^{V659E} IC_{50} values were greater than those of neratinib at 220 nmol/L and 1.17 μmol/L. *HER2*^{WT} IC_{50} values ranged from 1.10 to 15.38 μmol/L (Supplementary Fig. S8). Finally, we evaluated the *HER2*-mutation–dependent effects of trastuzumab in the five cPAC cell lines described above (two *HER2*^{V659E} and three *HER2*^{WT}) and the positive control cell line BT474 at doses ranging from 1×10^{-6} μg/mL to 1 mg/mL for 72 hours. Although trastuzumab did not decrease viability below 50% for any of the cell lines at 72 hours, the greatest dose-dependent responses were observed in the BT474 control line (65% viability at 10 μg/mL, consistent with prior publications) and in the *HER2*^{V659E} line OSUK9PAPADRex (74% viability at 10 μg/mL). More limited responses

were observed in OSUK9PAPADOscar (*HER2*^{V659E}) and OSUK9PADSnickers (*HER2*^{WT}) and no responses at any dose in Riley (*HER2*^{V659E}) and BACA (*HER2*^{WT}; Supplementary Fig. S9). Overall, these studies support that *HER2*^{V659E} in cPAC is an activating event that stabilizes HER2 homodimers and heterodimers, confers dependency on downstream signaling, and confers sensitivity to targeted HER2 tyrosine kinase inhibition.

Discussion

Through multiplatform next-generation sequencing of 88 naturally occurring primary canine NSCLC cases (77 tumors and 11 cell lines), we describe for the first time the detailed genomic underpinnings of this cancer. The cohort included major NSCLC subtypes occurring in dogs and humans: cPAC ($n = 74$, cPASC ($n = 11$), and cPSCC ($n = 3$; Supplementary Table S2; Supplementary Fig. S1). Although lung cancer may be overrepresented in Doberman pinschers, Australian shepherds, Irish setters, and Bernese mountain dogs (7), Labrador retrievers comprised the largest pure breed in this cohort (21%) followed by mixed breeds (25%). The cohort was gender balanced (52% females), primarily neutered/spayed (92%), and bore a median age at diagnosis of 11 years. Given that dogs are companion and service animals that typically share the same environment with humans, they may have a role to play as sentinels for human lung cancer environmental risk factors. Some data suggest that environmental risks are shared across species. For example, an increased risk of developing cPAC (OR: 2.4; CI 95%, 0.7–7.8; P = not given) trends toward association with having a smoker in the home in dogs with short (brachycephalic) or medium length (mesocephalic) noses, such as Labrador retrievers (26). Although secondhand smoke exposure in the dogs in our cohort is possible given that exposure was not recorded, genomic landscapes of human lung cancers in never-smokers have not been shown to differ based on exposure to secondhand smoke (27). Exposure to other environmental carcinogens such as air pollutants may also play a role in the development of lung cancers. For example, increased lung cancer risk may be present in dogs with higher amounts of carbon deposits known as anthracosis (OR: 2.1; CI 95%, 1.20–3.70; $P < 0.01$; ref. 28), although in humans anthracosis has been commonly observed in normal lungs as well as tumors and lymph nodes. In this cohort, anthracosis was recorded in 15 cases and pneumoconiosis (lung disease associated with pollutant exposure) in one case. However, no associations between anthracosis annotation and genetic features of these cases were observed. Overall, our studies included broad representation of lung cancer across histologic subtypes, breeds, ages, and pollutant exposures reflective of primary canine lung cancer diversity seen in the clinical setting in the United States. Overall, support exists for shared etiologies between canine and human never-smoker lung cancer, including secondhand smoke, organic dusts, and outdoor and indoor air pollution, suggesting that study of canine lung cancer can be informative for understanding human lung cancer risks and etiologies. Genomic characterization of canine lung cancers is a first major step toward understanding variables influencing lung cancer development in pet dogs.

Unique genomic characteristics of human never-smoker lung cancer include low somatic mutation burden, C:G>T:A enrichment, and activating mutations or fusions impacting *EGFR* (45%), *ALK* (5%–11%), *ROS* (1.5%–6%), *HER2* (3%–5%), and *RET* (2%; refs. 4, 29). Here, we also observed a low somatic burden of SNVs, CNVs, and SVs through exome sequencing in five matched tumor/normal cPAC pairs. We additionally observed that the most common mutation signature in these five cases was the age-associated COSMIC signature 1A in four of five (80%) similar to the enrichment seen in human NSCLC (Supplementary Fig. S3). This signature is associated with age in many human cancers, putatively the result of spontaneous deamination of 5-methyl-cytosine. COSMIC signature 2, associated with APOBEC cytidine deaminase activity, was also present in two cases. This signature is most prominently associated with cervical and bladder cancers, but is also commonly found in lung adenocarcinoma and SCC. Although these signatures are sometimes associated with *APOBEC* gene variants in human cancers (30), no putatively pathogenic germline or somatic *APOBEC* mutations were observed in this canine cohort. Based on our studies, primary canine lung cancers bear a low mutation burden (TMB mean of 2.04 mutations/Mb) and mutation signatures reflective of those seen in human never-smoker lung cancers.

The most common recurrently mutated genes containing somatic potentially pathogenic SNVs in the full cohort included *HER2* (31.5%), *TP53* (12.5%), *PTEN* (5.7%), *SMAD4* (4.5%), *KRAS* (4.5%), *VHL* (3.4%), and *HRAS* (2.3%). Recurrent *CDKN2A/B* focal deletions were also observed in two of five (40%) cases (Fig. 1A and B) along with a homozygous missense mutation, G50R, equivalent to human codon G101 mutations. *CDKN2A* deletions were the most common alteration by frequency, occurring at rates comparable with those in human NSCLC. Two focal deletions were observed out of five exome-sequenced cases, with signs of larger-scale CFA11 losses in remaining cases (Supplementary Fig. S2). *CDKN2A* is mutated in ~30% of all human NSCLC, primarily via homozygous deletion, and this number is reduced to around 25% in never-smokers. The next most common alterations after *CDKN2A* and *HER2* were *TP53* missense and truncating mutations comparable with DNA binding domain mutations in human *TP53*. Similar to human NSCLC, we observed a reduced burden of *TP53* mutations (12.4%, two stop gains and nine likely pathogenic missense mutations) relative to human smoker NSCLC in which more than half of tumors are mutated. *PTEN* mutations were the next most common at 5.6%. *PTEN* is mutated in ~9% of human NSCLC, but only ~2% of never-smoker NSCLC. We additionally identified four somatic mutations in the tumor suppressor *SMAD4*, mutated in ~5% of human NSCLC at comparable rates in smoker and never-smoker cancer. *KRAS* mutations are the most common oncogenic mutations in human smoker NSCLC (~30%–40% of cases), but occur at reduced frequencies in never-smoker lung cancer (0%–7%). *KRAS* mutations in our cohort were rare (2 G12V, 1 G12D, and 1 Q61K), but comparable to human hotspots. Canine *HRAS* missense mutations were also located in human-equivalent hotspots (Q61L and F78S). Additional likely pathogenic somatic mutations included individual cases of *AKT1* amplification, *KIT/KDR* amplification, *EGFR* A726T (human A755), *MET* M1269V (human M1268), and *VHL* P97L (human P97). *WWTR1*, the only COSMIC gene bearing a somatic translocation in exome-sequenced cases, has been shown to undergo translocation with *CAMTA1* in human epithelioid hemangioendothelioma (31). We identified a *WWTR1* translocation of unknown consequence with *ATP5F1*. Although we identified translocations occurring in coding regions in five exome-sequenced tumors, it remains possible that, as in human never-smoker lung cancer, *EML4–ALK* fusions,

ROS1 fusions, *RET* fusions, and other fusions may also be present in canine lung cancer.

In addition to charting the landscape of cPAC, we have found recurrent *KRAS* and *TP53* mutations in cPASC and provide a view of possible drivers in cPSCC. In cPASC, *HRAS* Q61L and *KRAS* Q61K each occurred in one case. Finally, although no recurrent mutations were identified in the three cPSCCs, we identified one case with somatic *BRAF* V588E (equivalent to the human V600E hotspot) and another bearing *PTPN11* G503V (equivalent to the human G503V hotspot).

HER2 contained the most somatic mutations with hotspot mutations occurring solely in cPAC (37.8%). *HER2* is a well-characterized human oncogene and drug target mutated in ~6% of all cancers based on cBioPortal query of 10,967 cases in the TCGA pan-cancer atlas (32, 33). Most alterations are focal amplifications, but activating point mutations and insertions are also common. In human NSCLC, *HER2* mutations are oncogenic drivers in ~1% to 4% of cases with mutations and insertions mostly in exon 20 at codon 776 resulting in constitutive HER2 kinase domain activation and downstream signaling through the PI3K and MAPK pathways (29, 34, 35). *HER2* may also be more commonly mutated in human never-smoker lung cancer, with point mutations at frequencies reported at 3% to 5% (36), predominately in female never-smokers who carry a median OS of ~2 years (35). *HER2* TMD polar mutations ($HER2^{V659E/D}$ and $HER2^{G660D}$) are present in 0.18% of human lung adenocarcinomas and are exclusive with *HER2* kinase domain mutations (37). Amplicon analysis capable of identification of point mutations and small insertions or deletions covered canine *HER2* exons 8 and 17 to 22 including transmembrane and kinase domains. Additionally, Sanger sequencing of all exons in five canine cell lines with WT *HER2* based on amplicon sequencing (OSUK9PAD, BACA, CLAC, K9PADSQ, and OSULSCC1) found no somatic *HER2* mutations in other sites (Supplementary Table S11). It is nonetheless possible that somatic mutations occurring in other regions of *HER2* were not identified in amplicon-sequenced samples even though data facilitating functional interpretation of these variants would be limited.

In addition to point mutations, *HER2* amplification has also been identified in ~1% of human NSCLC (29), with enrichment in EGFR-inhibitor–resistant tumors (38). Protein overexpression is reported in 6% to 35% of tumors, including up to 42% of adenocarcinomas, and correlates with poor prognosis (39–42). We detected no somatic *HER2* focal amplifications or numerical CFA9 gains in five exome-sequenced cases (Fig. 1B; Supplementary Fig. S2) or two previously aCGH-profiled cell lines. However, four of these seven cases contained somatic, putatively activating *HER2* SNVs. Given that *HER2* amplification/overexpression and SNVs are typically mutually exclusive, it remains possible that our broader amplicon cohort contained undetected *HER2* amplifications. We therefore utilized qRT-PCR and IHC studies to more broadly assess HER2 overexpression and did not find evidence for significant tumor-specific HER2 overexpression (Supplementary Figs. S5 and S6; Supplementary Table S13). Thus, it is unlikely that *HER2* is frequently amplified in canine lung cancer.

Overall, though we observed a similar mutation spectrum in canine lung cancer relative to human never-smoker NSCLC, the notable exception is abundance of *HER2* mutations and lack of *EGFR* mutations. EGFR mutations occur at low frequency in human smoker lung cancers (0%–7%), but are enriched in human never-smokers (~45%). Canine HER2 shares normal and oncogenic roles with human HER2 based on sequence conservation (92.2% protein identity) and prior study of its role in canine cell signaling. $HER2^{V659E}$ occurs at a highly conserved residue (100% identity in the TMD from amino acids 654–674) and to the *neu* (rat HER2) variant identified in a rat glioblastoma cell line that originally led to the discovery of *HER2*'s oncogene status (43). HER2 has previously been implicated in canine cancers via overexpression by IHC and qRT-PCR in canine mammary tumors (44), through its utility as a vaccine target in canine osteosarcoma (45), and through downstream signaling activation in canine lung cancer (10). Thus, HER2 sequence and pathway biology is conserved, so the predominance of *HER2* mutations as erbB signaling activators in lieu of *EGFR* mutations in cPAC may be the result of cell-of-origin and genetic background influences. Cell-of-origin determination in canine lung cancers is challenging because the pulmonary adenocarcinoma diagnosis includes tumors arising from primary, secondary, and tertiary bronchioles and thus topographic origin can be difficult to determine. However, evidence supports that HER2 is broadly important for canine pulmonary epithelium. For example, neuregulin-stimulated HER2 increases proliferation in pulmonary epithelial cells by activation of the JAK–STAT pathway. Further, when HER2 activation is blocked via antibodies to neuregulin or HER2 in a scratch wound-healing assay of pulmonary epithelial cells, wound closure is significantly delayed, suggesting HER2 activation is necessary for epithelial proliferation (46). We have also found that IHC of canine normal lung showed stronger HER2 staining of all bronchioalveolar regions when compared with EGFR staining of normal adult canine lung. These data suggest that HER2 may play a more central role than EGFR in canine alveolar and airway epithelial cells during chronic lung injury and for general proliferative processes. Prolonged activation could lead to cellular transformation and neoplasia. Further, *EGFR* mutations have been associated with particular histotypes; i.e., they are frequent in lepidic and acinar patterns and infrequent in mucinous patterns in female Asian never-smoker PAC. In this population, the most frequent adenocarcinoma histotype was acinar (142 cases, 71.7%), followed by papillary (18 cases, 9.1%), solid (17 cases, 8.6%), lepidic (9 cases, 4.5%), and micropapillary (1 case, 0.5%). Interestingly, our canine cohort had predominantly papillary morphology (69%), with only 5% acinar (5%). Therefore, differences in cell of origin in both species could account for the differences in *EGFR* mutation frequencies. Background genetic context likely also plays a primary role in shaping enrichment for *HER2* mutations in cPAC. This is also true in human lung cancer where *EGFR* mutation frequency varies by more than 3-fold between different human populations. The Asian population has a very high rate of *EGFR* mutation among the never-smoking population, up to 51.4% overall and as high as 64% in some populations such as the Kinh, versus about 20% in Caucasians (47–49). These differences in human populations suggest a sensitivity of *EGFR* mutations to genetic context. Conversely, *HER2* mutations are found in all human populations at about the same frequency, suggesting that *HER2* mutations in humans may not be as sensitive to genetic background.

We have additionally shown that *HER2* hotspot mutations can be detected in the plasma of dogs bearing $HER2^{V659E}$ cPACs even at early disease stages (Fig. 1E; Supplementary Table S12). In human NSCLC, ctDNA has been shown to be significantly enriched in plasma relative to controls with key genetic features

identifiable via liquid biopsy. Associations have been found between ctDNA levels and tumor stage, grade, lymph node status, metastatic sites, response, and survival (50, 51). The first FDA-approved liquid biopsy test was the cobas EGFR Mutation Test v2, a real-time PCR assay utilized in NSCLC for the detection of *EGFR* exon 18 to 21 mutations in tissue or plasma to guide EGFR inhibitor treatment assignment (52, 53). Our proof-of-principle study supports that ctDNA is also detectable in primary canine lung cancer patient plasma. A noninvasive *HER2*^{V659E} assay will enable genotyping patients when tumor tissue is limited and may have a role in treatment monitoring or detection of minimal residual disease. This assay will also facilitate prospective analysis of *HER2*^{V659E}'s diagnostic and prognostic value.

In human cancers, *HER2* TMD mutations constitutively activate prosurvival HER2 signaling (37) and are associated with HER2 inhibitor responses (23). We have confirmed in this study that, similar to human *HER2* TMD mutants, canine *HER2*^{V659E} cell lines constitutively activate downstream signaling through AKT and are selectively sensitive to the HER2 TKI inhibitors neratinib and lapatinib *in vitro* (Fig. 2; Supplementary Fig. S7). In order to further assess the role of dimerization in HER2 activation in cPAC, we also performed drug-dose–response studies for erlotinib and trastuzumab (Supplementary Figs. S8 and S9). One of two *HER2*-mutant cell lines showed erlotinib sensitivity. Trastuzumab responses were poor overall and did not correlate with HER2 status, although dose–response relationships were observed in three of five cell lines. Trastuzumab's human binding site is highly conserved in canine (only a single amino acid difference) and trastuzumab has been shown to bind canine HER2 and inhibit proliferation of HER2-overexpressing canine cancer cell lines (54). However, even the human *HER2*-amplified cell line BT474 did not show viability reduction below 50% in our hands. It is likely that the effects of trastuzumab on CellTiter-Glo viability are broadly muted at the 72-hour time points we utilized. Overall, these studies indicate that HER2^{V659E} in cPAC is an activating event that stabilizes HER2 homodimers and heterodimers, confers dependency on downstream signaling, and confers sensitivity to targeted HER2 tyrosine kinase inhibition. We have charted the genomic landscape of primary canine lung cancers including the NSCLC subtypes cPAC, cPASC, and cPSCC. We have identified recurrent *HER2* mutations in these cancers and present, to our knowledge, the first complete suite of evidence supporting an oncogenic role for and dependency on constitutively activating mutations in *HER2* in a canine cancer. Further work is needed to exhaustively profile these tumors, particularly according to variation across breeds and through integration of additional data types including epigenomics, RNA-seq, and proteomics. However, these data nonetheless offer significant immediate diagnostic and therapeutic opportunities for dogs with primary lung cancer and aid comparative understanding of never-smoker and *HER2*-mutant lung cancer. These findings set the stage for HER2 inhibitor toxicity, dose-finding, and efficacy studies in dogs that will guide utilization of HER2 inhibitors in the veterinary clinic.

Disclosure of Potential Conflicts of Interest

S.L. Sinicropi-Yao is an employee of Sanofi. M. Murtaza reports receiving commercial research grants from Ethos Discovery. W.P.D. Hendricks is a consultant/advisory board member for The One Health Company. No potential conflicts of interest were disclosed by the other authors.

Authors' Contributions

Conception and design: G. Lorch, M. Murtaza, J. Trent, D.P. Carbone, W.P.D. Hendricks
Development of methodology: G. Lorch, K. Sivaprakasam, V. Zismann, M.J. Koenig, M. Murtaza, W.P.D. Hendricks
Acquisition of data (provided animals, acquired and managed patients, provided facilities, etc.): G. Lorch, V. Zismann, N. Perdigones, S. Facista, S. Wong, W.S. Liang, J.M. Amann, S.L. Sinicropi-Yao, M.J. Koenig, K.L. Perle, M. Murtaza
Analysis and interpretation of data (e.g., statistical analysis, biostatistics, computational analysis): G. Lorch, K. Sivaprakasam, N. Perdigones, A. Nazareno, S. Wong, K. Drenner, M.J. Koenig, K.L. Perle, T.G. Whitsett, M. Murtaza, D.P. Carbone
Writing, review, and/or revision of the manuscript: G. Lorch, K. Sivaprakasam, V. Zismann, N. Perdigones, J.M. Amann, K.L. Perle, T.G. Whitsett, M. Murtaza, J. Trent, D.P. Carbone, W.P.D. Hendricks
Administrative, technical, or material support (i.e., reporting or organizing data, constructing databases): G. Lorch, N. Perdigones, J. Trent, W.P.D. Hendricks
Study supervision: G. Lorch, V. Zismann, J. Trent, D.P. Carbone, W.P.D. Hendricks
Other (running a subset of the samples that generated data for this publication): T. Contente-Cuomo

Acknowledgments

This study was supported by National Canine Cancer Foundation GL150H-005 (G. Lorch), the Bisgrove Scholars Program (M. Murtaza), philanthropic support to the TGen Foundation (J. Trent and W. Hendricks), CTSA UL1TR001070 (G. Lorch), NCI P30 CA016058 (G. Lorch, J. Trent, and W. Hendricks), Brooke's Blossoming Hope (J. Trent and W. Hendricks). We thank Dr. Amy LeBlanc, Director of the NCI's Comparative Oncology Program (COP), and Christina Mazcko, COP Program Manager, for their assistance with CCOGC sample procurement and annotation. Additionally, we thank Dr. Holly Borghese of the OSU CVM Veterinary Biospecimen Repository for her expertise in sample procurement and Dr. Kurtis Yearsley of the OSU Pathology Imaging Core for his expertise in quantitative image analysis. We thank Drs. Alshad Lalani, Irmina Diala, and Lisa Eli of Puma Biotechnology for fruitful discussion of HER2 inhibition and provision of neratinib for this study.

The costs of publication of this article were defrayed in part by the payment of page charges. This article must therefore be hereby marked *advertisement* in accordance with 18 U.S.C. Section 1734 solely to indicate this fact.

Received April 4, 2019; revised June 19, 2019; accepted July 29, 2019; published first August 20, 2019.

References

1. Wilson DW. Tumors of the respiratory tract. In: Meuten DJ, editor. Tumors in domestic animals. 5th ed. John Wiley & Sons; 2017. p467–98.
2. Clément-Duchêne C, Wakelee H. Lung cancer incidence in never smokers. European J Clin Med Oncol 2010;2:53.
3. Samet JM, Avila-Tang E, Boffetta P, Hannan LM, Olivo-Marston S, Thun MJ, et al. Lung cancer in never smokers: clinical epidemiology and environmental risk factors. Clin Cancer Res 2009;15:5626–45.
4. Govindan R, Ding L, Griffith M, Subramanian J, Dees ND, Kanchi KL, et al. Genomic landscape of non-small cell lung cancer in smokers and never-smokers. Cell 2012;150:1121–34.
5. Hellmann MD, Ciuleanu TE, Pluzanski A, Lee JS, Otterson GA, Audigier-Valette C, et al. Nivolumab plus ipilimumab in lung cancer with a high tumor mutational burden. N Engl J Med 2018;378:2093–104.

6. Hahn FF, Muggenburg BA, Griffith WC, editor. Primary lung cancer in the longevity study/control population of the ITRI beagle dog colony. Springfield, VA: National Technical Information Service; 1992. 133–6p.
7. Griffey SM, Kraegel SA, Madewell BR. Rapid detection of K-ras gene mutations in canine lung cancer using single-strand conformational polymorphism analysis. Carcinogenesis 1998;19:959–63.
8. Kraegel SA, Gumerlock PH, Dungworth DL, Oreffo VI, Madewell BR. K-ras activation in non-small cell lung cancer in the dog. Cancer Res 1992;52: 4724–7.
9. Tierney LA, Hahn FF, Lechner JF. p53, erbB-2 and K-ras gene alterations are rare in spontaneous and plutonium-239-induced canine lung neoplasia. Radiat Res 1996;145:181–7.
10. Mariotti ET, Premanandan C, Lorch G. Canine pulmonary adenocarcinoma tyrosine kinase receptor expression and phosphorylation. BMC Vet Res 2014;10:19.
11. Gordon I, Paoloni M, Mazcko C, Khanna C. The Comparative Oncology Trials Consortium: using spontaneously occurring cancers in dogs to inform the cancer drug development pathway. PLoS Med 2009;6: e1000161.
12. Murtaza M, Dawson SJ, Pogrebniak K, Rueda OM, Provenzano E, Grant J, et al. Multifocal clonal evolution characterized using circulating tumour DNA in a case of metastatic breast cancer. Nat Commun 2015;4:8760.
13. Li H, Handsaker B, Wysoker A, Fennell T, Ruan J, Homer N, et al. The sequence alignment/map format and SAMtools. Bioinformatics 2009;25: 2078–9.
14. Hsu WL, Huang HM, Liao JW, Wong ML, Chang SC. Increased survival in dogs with malignant mammary tumours overexpressing HER-2 protein and detection of a silent single nucleotide polymorphism in the canine HER-2 gene. Vet J 2009;180:116–23.
15. Forbes SA, Beare D, Boutselakis H, Bamford S, Bindal N, Tate J, et al. COSMIC: somatic cancer genetics at high-resolution. Nucleic Acids Res 2017;45:D777–D83.
16. Alexandrov LB, Nik-Zainal S, Wedge DC, Aparicio SA, Behjati S, Biankin AV, et al. Signatures of mutational processes in human cancer. Nature 2013;500:415.
17. Gehring JS, Fischer B, Lawrence M, Huber W. SomaticSignatures: inferring mutational signatures from single-nucleotide variants. Bioinformatics 2015;31:3673–5.
18. Sherry ST, Ward M-H, Kholodov M, Baker J, Phan L, Smigielski EM, et al. dbSNP: the NCBI database of genetic variation. Nucleic Acids Res 2001;29: 308–11.
19. Bai B, Zhao W-M, Tang B-X, Wang Y-Q, Wang L, Zhang Z, et al. DoGSD: the dog and wolf genome SNP database. Nucleic Acids Res 2014;43: D777–D83.
20. Liu C, Cui H, Gu D, Zhang M, Fang Y, Chen S, et al. Genetic polymorphisms and lung cancer risk: Evidence from meta-analyses and genome-wide association studies. Lung Cancer 2017;113:18–29.
21. Perdigones N, Murtaza M. Capturing tumor heterogeneity and clonal evolution in solid cancers using circulating tumor DNA analysis. Pharmacol Ther 2017;174:22–6.
22. Suzawa K, Toyooka S, Sakaguchi M, Morita M, Yamamoto H, Tomida S, et al. Antitumor effect of afatinib, as a human epidermal growth factor receptor 2-targeted therapy, in lung cancers harboring HER2 oncogene alterations. Cancer Sci 2016;107:45–52.
23. Ou SI, Schrock AB, Bocharov EV, Klempner SJ, Haddad CK, Steinecker G, et al. HER2 transmembrane domain (TMD) mutations (V659/G660) that stabilize homo- and heterodimerization are rare oncogenic drivers in lung adenocarcinoma that respond to afatinib. J Thorac Oncol 2017;12: 446–57.
24. Clemente-Vicario F, Alvarez CE, Rowell JL, Roy S, London CA, Kisseberth WC, et al. Human genetic relevance and potent antitumor activity of heat shock protein 90 inhibition in canine lung adenocarcinoma cell lines. PLoS One 2015;10:e0142007.
25. Canonici A, Gijsen M, Mullooly M, Bennett R, Bouguern N, Pedersen K, et al. Neratinib overcomes trastuzumab resistance in HER2 amplified breast cancer. Oncotarget 2013;4:1592.
26. Reif JS, Dunn K, Ogilvie GK, Harris CK. Passive smoking and canine lung cancer risk. Am J Epidemiol 1992;135:234–9.
27. Couraud S, Debieuvre D, Moreau L, Dumont P, Margery J, Quoix E, et al. No impact of passive smoke on the somatic profile of lung cancers in never-smokers. Eur Respir J 2015;45:1415–25.
28. Bettini G, Morini M, Marconato L, Marcato PS, Zini EJTVJ. Association between environmental dust exposure and lung cancer in dogs. Vet J 2010; 186:364–9.
29. Campbell JD, Alexandrov A, Kim J, Wala J, Berger AH, Pedamallu CS, et al. Distinct patterns of somatic genome alterations in lung adenocarcinomas and squamous cell carcinomas. Nat Genet 2016;48:607–16.
30. Nik-Zainal S, Wedge DC, Alexandrov LB, Petljak M, Butler AP, Bolli N, et al. Association of a germline copy number polymorphism of APOBEC3A and APOBEC3B with burden of putative APOBEC-dependent mutations in breast cancer. Nat Genet 2014;46:487–91.
31. Errani C, Zhang L, Sung YS, Hajdu M, Singer S, Maki RG, et al. A novel WWTR1CAMTA1 gene fusion is a consistent abnormality in epithelioid hemangioendothelioma of different anatomic sites. Genes Chromosomes Cancer 2011;50:644–53.
32. Gao J, Aksoy BA, Dogrusoz U, Dresdner G, Gross B, Sumer SO, et al. Integrative analysis of complex cancer genomics and clinical profiles using the cBioPortal. Sci Signal 2013;6:pl1.
33. Weinstein JN, Collisson EA, Mills GB, Shaw KRM, Ozenberger BA, Ellrott K, et al. The cancer genome atlas pan-cancer analysis project. Nat Genet 2013; 45:1113–20.
34. Mazieres J, Peters S, Lepage B, Cortot AB, Barlesi F, Beau-Faller M, et al. Lung cancer that harbors an HER2 mutation: epidemiologic characteristics and therapeutic perspectives. J Clin Oncol 2013;31:1997–2003.
35. Mazieres J, Barlesi F, Filleron T, Besse B, Monnet I, Beau-Faller M, et al. Lung cancer patients with HER2 mutations treated with chemotherapy and HER2-targeted drugs: results from the European EUHER2 cohort. Ann Oncol 2016;27:281–6.
36. Shigematsu H, Takahashi T, Nomura M, Majmudar K, Suzuki M, Lee H, et al. Somatic mutations of the HER2 kinase domain in lung adenocarcinomas. Cancer Res 2005;65:1642–6.
37. Pahuja KB, Nguyen TT, Jaiswal BS, Prabhash K, Thaker TM, Senger K, et al. Actionable activating oncogenic ERRB2/HER2 transmembrane and juxtamembrane domain mutations. Cancer Cell 2018;34:792–806.
38. Takezawa K, Pirazzoli V, Arcila ME, Nebhan CA, Song X, de Stanchina E, et al. HER2 amplification: a potential mechanism of acquired resistance to EGFR inhibition in EGFR-mutant lung cancers that lack the second-site EGFRT790M mutation. Cancer Discov 2012;2(10):922–33.
39. Pellegrini C, Falleni M, Marchetti A, Cassani B, Miozzo M, Buttitta F, et al. HER-2/Neu alterations in non-small cell lung cancer: a comprehensive evaluation by real time reverse transcription-PCR, fluorescence in situ hybridization, and immunohistochemistry. Clin Cancer Res 2003;9: 3645–52.
40. Rouquette I, Lauwers-Cances V, Allera C, Brouchet L, Milia J, Nicaise Y, et al. Characteristics of lung cancer in women: importance of hormonal and growth factors. Lung Cancer 2012;76:280–5.
41. Langer CJ, Stephenson P, Thor A, Vangel M, Johnson DH. Trastuzumab in the treatment of advanced non-small-cell lung cancer: is there a role? Focus on Eastern Cooperative Oncology Group study 2598. J Clin Oncol 2004; 22:1180–7.
42. Lara Jr PN, Laptalo L, Longmate J, Lau DH, Gandour-Edwards R, Gumerlock PH, et al. Trastuzumab plus Docetaxel in HER2/neu–positive non–small-cell lung cancer: A California Cancer Consortium Screening and Phase II Trial. Clin Lung Cancer 2004;5:231–6.
43. Bargmann CI, Hung MC, Weinberg RA. Multiple independent activations of the neu oncogene by a point mutation altering the transmembrane domain of p185. Cell 1986;45:649–57.
44. Gama A, Alves A, Schmitt F. Identification of molecular phenotypes in canine mammary carcinomas with clinical implications: application of the human classification. Virchows Arch 2008;453:123–32.
45. Mason NJ, Gnanandarajah JS, Engiles JB, Gray F, Laughlin D, Gaurnier-Hausser A, et al. Immunotherapy with a HER2-targeting listeria induces HER2-specific immunity and demonstrates potential therapeutic effects in a phase I trial in canine osteosarcoma. Clin Cancer Res 2016;22: 4380–90.
46. Vermeer PD, Einwalter LA, Moninger TO, Rokhlina T, Kern JA, Zabner J, et al. Segregation of receptor and ligand regulates activation of epithelial growth factor receptor. Nature 2003;422:322–6.

47. Yatabe Y, Kerr KM, Utomo A, Rajadurai P, Tran VK, Du X, et al. EGFR mutation testing practices within the Asia Pacific region: results of a multicenter diagnostic survey. J Thorac Oncol 2015;10:438–45.
48. Shigematsu H, Lin L, Takahashi T, Nomura M, Suzuki M, Wistuba II, et al. Clinical and biological features associated with epidermal growth factor receptor gene mutations in lung cancers. J Natl Cancer Inst 2005;97: 339–46.
49. Shi Y, Au JS, Thongprasert S, Srinivasan S, Tsai CM, Khoa MT, et al. A prospective, molecular epidemiology study of EGFR mutations in Asian patients with advanced non-small-cell lung cancer of adenocarcinoma histology (PIONEER). J Thorac Oncol 2014;9:154–62.
50. Nie K, Jia Y, Zhang XJ. Cell-free circulating tumor DNA in plasma/serum of non-small cell lung cancer. Tumour Biol 2015;36:7–19.
51. Jiang T, Ren S, Zhou C. Role of circulating-tumor DNA analysis in non-small cell lung cancer. Lung Cancer 2015;90:128–34.
52. Kwapisz D. The first liquid biopsy test approved. Is it a new era of mutation testing for non-small cell lung cancer? Ann Transl Med 2017;5:46.
53. Wu Y-L, Zhou C, Liam C-K, Wu G, Liu X, Zhong Z, et al. First-line erlotinib versus gemcitabine/cisplatin in patients with advanced EGFR mutation-positive non-small-cell lung cancer: analyses from the phase III, randomized, open-label, ENSURE study. Ann Oncol 2015;26:1883–9.
54. Singer J, Weichselbaumer M, Stockner T, Mechtcheriakova D, Sobanov Y, Bajna E, et al. Comparative oncology: ErbB-1 and ErbB-2 homologues in canine cancer are susceptible to cetuximab and trastuzumab targeting. Mol Immunol 2012;50:200–9.